Supplementary information for

A biomolecular magnetic switch by diamagnetic cations

Haijun Yang[1#], Liuhua Mu[2,3#], Lei Zhang[4#], Zixin Wang[5], Shiqi Sheng[6], Jihong Wang[6], Hanxiao Chen[4], Yongshun Song[6], Jie Jiang[7], Peng Xiu[2,8], Wei Tong[4], Yueyu Zhang[2], Sanzhao Song[2], Nian Zhang[1], Jiefeng Cao[1], Fangyuan Zhu[1], Limin Zhou[1], Lijuan Zhang[1], Guosheng Shi[2,9], Jun Hu[1], Yong Wang[1], Xin Zhang[4*], Feng Zhang[5,2*], Haiping Fang[6,2,10*]

[1.]Shanghai Advanced Research Institute, Chinese Academy of Sciences, Shanghai, China.

[2.]Wenzhou Institute, University of Chinese Academy of Sciences, Wenzhou, China.

[3.]School of Physical Science, University of Chinese Academy of Sciences, Beijing, China.

[4.]High Magnetic Field Laboratory, Key Laboratory of High Magnetic Field and Ion Beam Physical Biology, HFIPS, Chinese Academy of Sciences, Hefei, China.

[5.]Key Laboratory of Optical Technology and Instrument for Medicine, Ministry of Education, University of Shanghai for Science and Technology, Shanghai, China.

[6.]School of Physics, East China University of Science and Technology, Shanghai, China.

[7.]School of Physical Science and Technology, Ningbo University, Ningbo, China.

[8.]Department of Engineering Mechanics, Zhejiang University, Hangzhou, China.

[9.]Shanghai Applied Radiation Institute, Shanghai University, Shanghai, China.

[10.]Shanghai Institute of Applied Physics, Chinese Academy of Sciences, Shanghai, China.

[#]These authors contributed equally to this work.

*Corresponding authors. Emails: fanghaiping@sinap.ac.cn; fzhang@usst.edu.cn; xinzhang@hmfl.ac.cn

Content

Supplementary Table 1| Concentration of Fe, Co and Ni in the AYFFF peptide assemblies*.

Sample	Concentration (ppb)								
	Fe			Co			Ni		
Peptide	N.D.	N.D.	0.3	N.D.	N.D.	N.D.	1.4	0.8	1.1
Peptide + $MgCl_2$	28.3	35.2	59.8	N.D.	0.2	0.1	N.D.	N.D.	N.D.
Peptide + $ZnCl_2$	N.D.	N.D.	N.D.	N.D.	N.D.	N.D.	59.2	54.9	58.2

* N.D. = not detected. The concentration of Fe, Co and Ni in the supernatant of peptide assemblies is extremely low (at or below the ppb level), demonstrating that the exceptionally strong paramagnetism of peptide assemblies does not come from these ferromagnetic impurities.

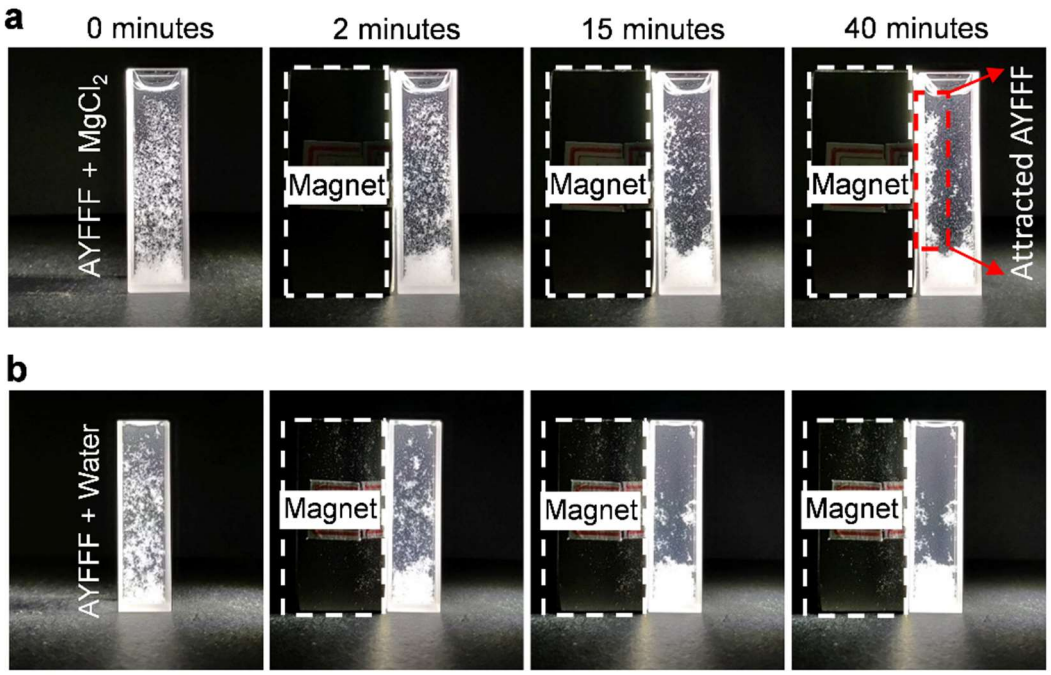

Supplementary Fig. 1| Dynamic adsorption of AYFFF peptide assemblies near a regular magnet in a 40 mM $MgCl_2$ solution. The white dashed frame outlines the edge of the magnet. The AYFFF peptide assemblies can be attracted toward the magnet with a surface magnetic field of 0.5 T (**a**), which further proved their exceptionally strong paramagnetism. As expected, in ultrapure water, the peptide assemblies were pushed away from the magnet due to their diamagnetism nature (**b**).

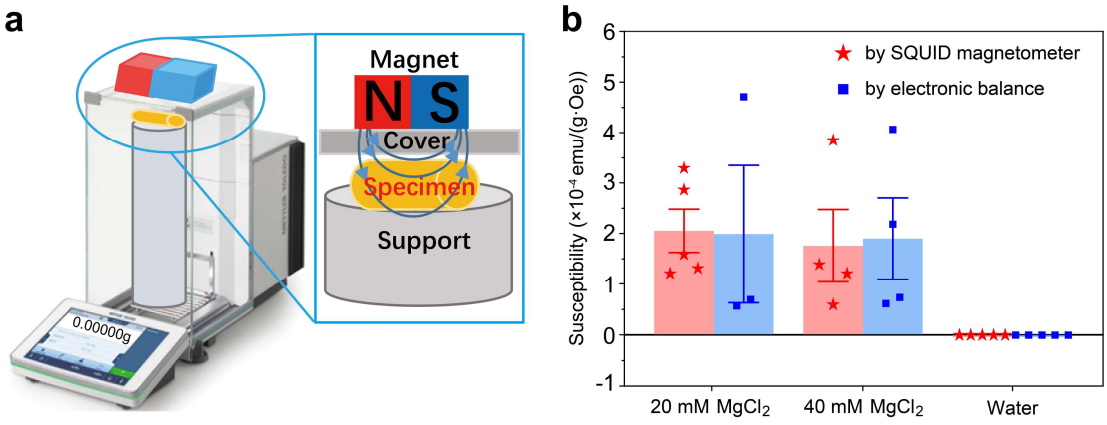

Supplementary Fig. 2| Measurements of mass susceptibility (χ) via a high-precision electronic balance. a, Schematic diagram of the experimental setup. To ensure the accuracy and repeatability of all the measurements, the magnetic field was kept constant by fixing the positions of the magnet on top of the balance cover and of the specimen on the support. **b**, χ of AYFFF peptide assemblies in 20 mM and 40 mM $MgCl_2$ solutions, together with water as a reference. Data are shown as mean ± SEM, together with symbols.

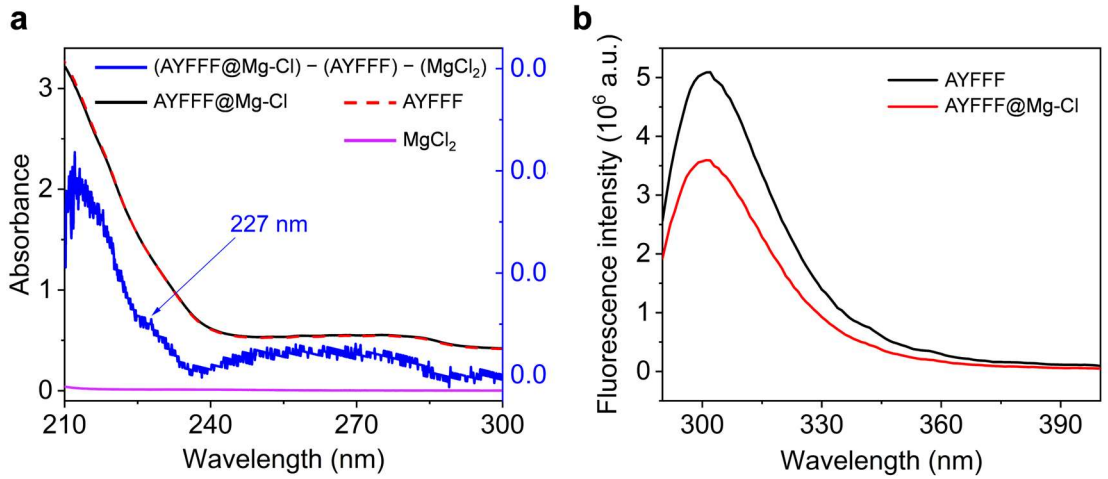

62

63 **Supplementary Fig. 3| Evidences for the existence of cation–π interactions between**
64 **magnesium cations and AYFFF. a,** UV absorption spectra of AYFFF (red dashed
65 line), AYFFF@Mg-Cl (black solid line) and $MgCl_2$ (purple solid line), together with
66 the difference spectrum of (AYFFF@Mg-Cl) – (AYFFF) – ($MgCl_2$) (blue solid line).
67 AYFFF@Mg-Cl represents the AYFFF assemblies in the $MgCl_2$ solution. There is a
68 weak positive band near 227 nm in the difference spectrum of (AYFFF@Mg-Cl) –
69 (AYFFF) – ($MgCl_2$) (blue line), which can be attributed to the cation–π interactions
70 between Mg^{2+} cations and aromatic rings in AYFFF assemblies. **b,** Fluorescence
71 spectra of the supernatant of AYFFF assemblies in a 40 mM $MgCl_2$ solution (red solid
72 line) and ultrapure water (black solid line). It shows an emission peak at 303 nm (as
73 excited at 275 nm), which could be assigned to the aromatic ring in the AYFFF
74 component that easily generated the π-π* transition. The fluorescence intensity of the
75 AYFFF supernatant dramatically weakened in a 40 mM $MgCl_2$ solution compared with
76 ultrapure water, indicating that the conjugated double bonds of aromatic rings in
77 AYFFF are greatly affected in the $MgCl_2$ solution.

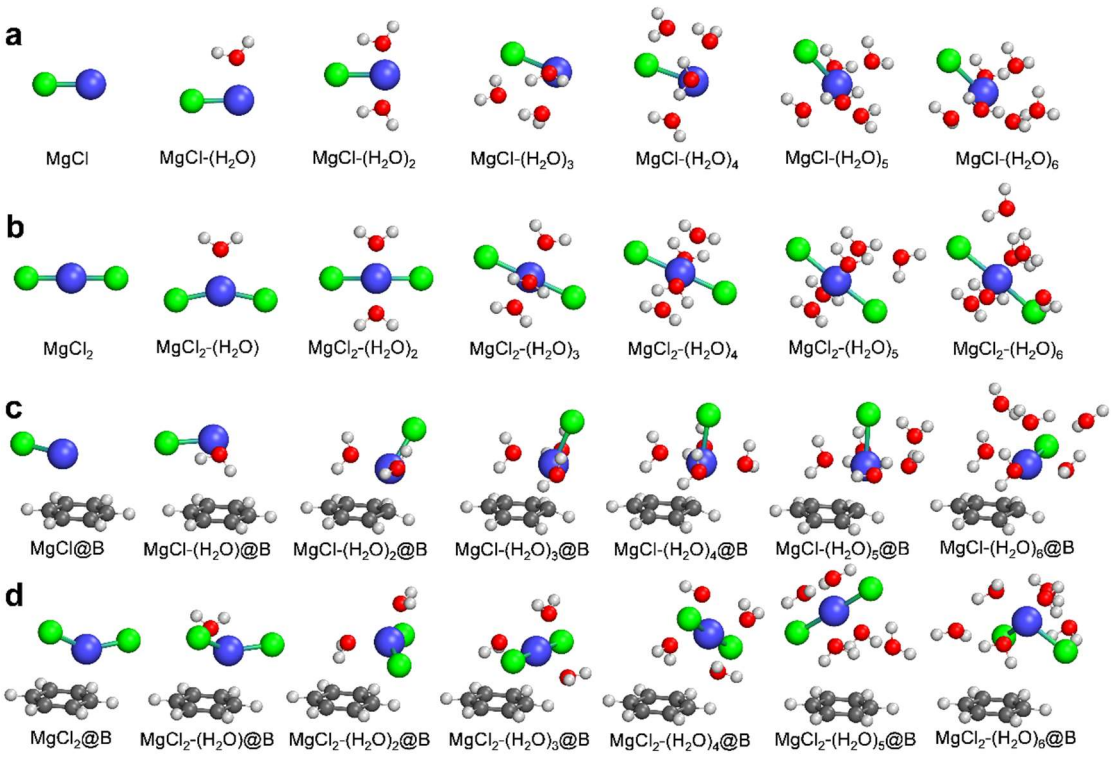

Supplementary Fig. 4| Stable optimized geometries of the hydrated MgCl (denoted as MgCl-$(H_2O)_n$) and $MgCl_2$ clusters (denoted as $MgCl_2$-$(H_2O)_n$) adsorbed on a benzene molecule (denoted as MgCl-$(H_2O)_n$@B and $MgCl_2$-$(H_2O)_n$@B, respectively). a, MgCl-$(H_2O)_n$. **b,** $MgCl_2$-$(H_2O)_n$. **c,** MgCl-$(H_2O)_n$@B. **d**, $MgCl_2$-$(H_2O)_n$@B. Spheres in green, blue, gray, red and white represent chloride, magnesium, carbon, oxygen and hydrogen, respectively. In the case of MgCl-$(H_2O)_6$@B, the magnesium cation directly interacts with the benzene molecule (**c**). While for $MgCl_2$-$(H_2O)_6$@B, water molecules are existing between the magnesium cation and benzene (**d**), indicating that the magnesium cation does not directly interact with benzene (i.e., their interaction is mediated by water). These results suggest that the interaction between the hydrated MgCl and benzene molecule is comparable to that between the hydrated $MgCl_2$ and benzene molecule.

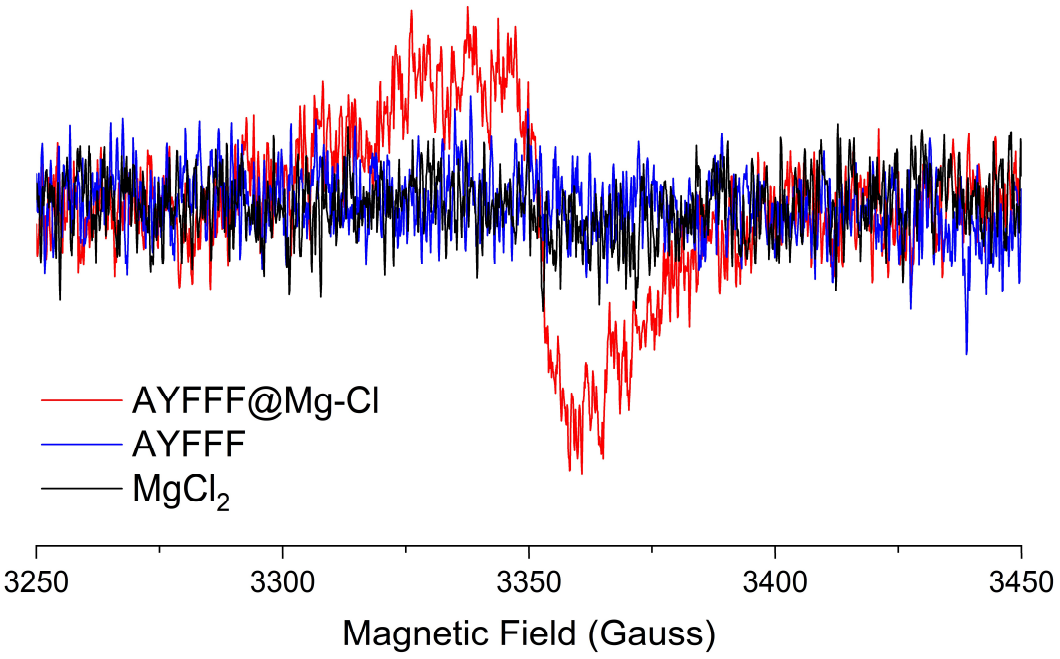

91

92 **Supplementary Fig. 5| Electron paramagnetic resonance (EPR) of AYFFF@Mg-**
93 **Cl, AYFFF and $MgCl_2$.** X-band (9.39 GHz) EPR spectrum was measured at 2 K, and
94 the g value of AYFFF@Mg-Cl is 2.003.